Article

From Microporous Regular Frameworks to Mesoporous Materials with Ultrahigh Surface Area: Dynamic Reorganization of Porous Polymer Networks

Pierre Kuhn, Aure#lien Forget, Dangsheng Su, Arne Thomas, and Markus Antonietti

J. Am. Chem. Soc., **2008**, 130 (40), 13333-13337 • DOI: 10.1021/ja803708s • Publication Date (Web): 13 September 2008

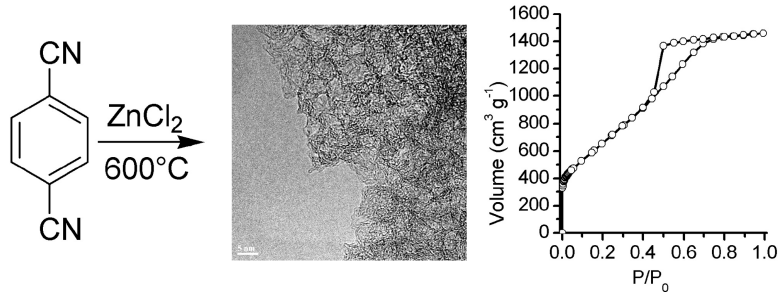

More About This Article

Additional resources and features associated with this article are available within the HTML version:

- Supporting Information
- Links to the 1 articles that cite this article, as of the time of this article download
- Access to high resolution figures
- Links to articles and content related to this article
- Copyright permission to reproduce figures and/or text from this article

View the Full Text HTML

Journal of the American Chemical Society is published by the American Chemical Society. 1155 Sixteenth Street N.W., Washington, DC 20036

J|A|C|S
ARTICLES

Published on Web 09/13/2008

From Microporous Regular Frameworks to Mesoporous Materials with Ultrahigh Surface Area: Dynamic Reorganization of Porous Polymer Networks

Pierre Kuhn,*,† Aurélien Forget,† Dangsheng Su,‡ Arne Thomas,† and Markus Antonietti†

Max Planck Institute of Colloids and Interfaces, Department of Colloid Chemistry, Research Campus Golm, 14424 Potsdam, Germany, and Fritz Haber Institute of the Max Planck Society, Department of Inorganic Chemistry, Faradayweg 4-6, 14195 Berlin, Germany

Received May 19, 2008; E-mail: kuhn@mpikg.mpg.de

Abstract: High surface area organic materials featuring both micro- and mesopores were synthesized under ionothermal conditions via the formation of polyaryltriazine networks. While the polytrimerization of nitriles in zinc chloride at 400 °C produces microporous polymers, higher reaction temperatures induce the formation of additional spherical mesopores with a narrow dispersity. The nitrogen-rich carbonaceous polymer materials thus obtained present surface areas and porosities up to 3300 $m^2\ g^{-1}$ and 2.4 $cm^3\ g^{-1}$, respectively. The key point of this synthesis relies on the occurrence of several high temperature polymerization reactions, where irreversible carbonization reactions coupled with the reversible trimerization of nitriles allow the reorganization of the dynamic triazine network. The $ZnCl_2$ molten salt fulfills the requirement of a high temperature solvent, but is also required as catalyst. Thus, this dynamic polymerization system provides not only highly micro- and mesoporous materials, but also allows controlling the pore structure in amorphous organic materials.

Introduction

In recent years, the development of new porous materials, especially micro- and mesoporous materials, opened unprecedented opportunities for a wide range of applications.[1] In order to extend the performance of such materials, increasing efforts are undertaken now toward the development of scaffolds containing organic building blocks, which due to their functional diversity would allow for an exquisite control over the chemical nature of the surface areas and the physical properties of the resulting networks.[2−4] Purely organic, micro- and mesoporous materials are however still a contemporary field of research.[5−7] Among all the possible synthetic strategies that can be employed for designing such materials, dynamic covalent chemistry (DCC) seems most promising.[8] Indeed, DCC is essential for the generation of robust crystalline porous architectures with a well-defined pore structure (due to self-organization allowed by dynamic reactions), in whom the building blocks are linked through strong covalent bonds.[9] However, most of the DCC reactions that could be relevant for the conception of porous structures (i.e., generating rigid bonds) rely on condensation reactions that yield moisture-sensitive materials.

Although the synthesis of crystalline inorganic materials largely relies on dynamic polymerization processes, only a few examples are known employing dynamic polymerizations for the generation of crystalline organic frameworks.[9,10] In such materials, the size and the shape of the pores are controlled, being determined by the crystal structure. On the other hand, it is still unclear if a dynamic polymerization could provide well-defined porous structures in *amorphous* organic materials.

Recently, we introduced a new dynamic polymerization system that allows the formation of porous crystalline or amorphous triazine based frameworks, through the reversible ionothermal trimerization of aromatic polynitriles.[10] (See Scheme 1.) Hence, highly porous organic materials with high thermal and chemical stability could be prepared conveniently and from simple monomers. Herein we show that consecutive irreversible reactions from those triazine-based microporous scaffolds lead to a structural evolution, which apparently occurs in a self-organized fashion, thus resulting in the formation of multimodal micro- and mesoporous materials with ultrahigh surface areas

† Max Planck Institute of Colloids and Interfaces.
‡ Fritz Haber Institute.

(1) Davis, B. H.; Sing, K. S. W. In *Handbook of porous solids*; Schüth, F.; Sing, K. S. W.; Weitkamp, J., Eds.; Wiley-VCH: Weinheim, Germany, 2002; Vol. 1, pp 3−34.
(2) Jones, C. W. *Science* **2003**, *300*, 439–440.
(3) Hatton, B.; Landskron, K.; Whitnall, W.; Perovic, D.; Ozin, G. A. *Acc. Chem. Res.* **2005**, *38*, 305–312.
(4) Papaefstathiou, G. S.; MacGillivray, L. R. *Coord. Chem. Rev.* **2003**, *246*, 169–184.
(5) Thomas, A.; Goettmann, F.; Antonietti, M. *Chem. Mater.* **2008**, *20*, 738–755.
(6) Weder, C. *Angew. Chem., Int. Ed.* **2008**, *47*, 448–450.
(7) Mastalerz, M. *Angew. Chem., Int. Ed.* **2008**, *47*, 445–447.
(8) Rowan, S. J.; Cantrill, S. J.; Cousins, G. R. L.; Sanders, J. K. M.; Stoddart, J. F. *Angew. Chem., Int. Ed.* **2002**, *41*, 898–952.
(9) Cote, A. P.; Benin, A. I.; Ockwig, N. W.; O'Keeffe, M.; Matzger, A. J.; Yaghi, O. M. *Science* **2005**, *310*, 1166–1170.
(10) Kuhn, P.; Antonietti, M.; Thomas, A. *Angew. Chem., Int. Ed.* **2008**, *47*, 3450–3453.

10.1021/ja803708s CCC: $40.75

Scheme 1. Reaction Scheme of the Dynamic Trimerization of Terephthalonitrile Leading to Formation of a 2D Framework with 1.5 nm Channels

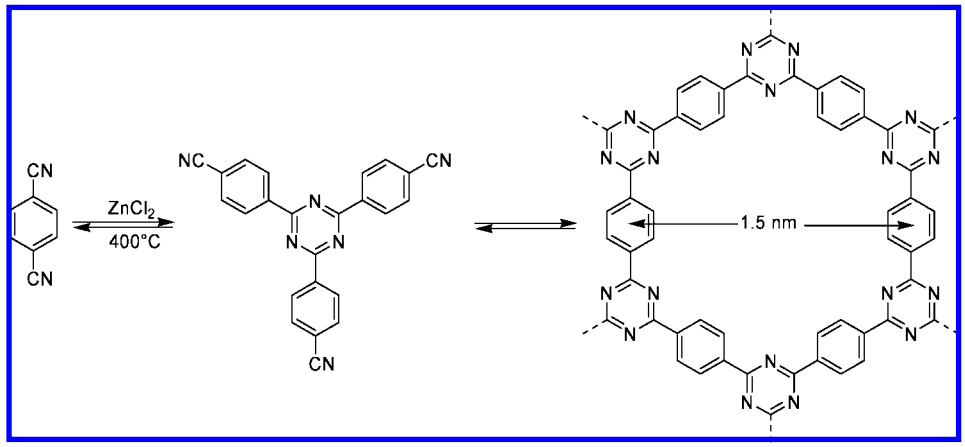

and porosities, containing well-defined mesopore sizes on more than one length scale.

Experimental Section

Chemicals. Zinc chloride (ABCR, anhydrous, 98%) was stored in a glovebox and used as received. 1,4-Dicyanobenzene (DCB) was purchased from Aldrich and was used as received.

Characterization. Elemental analyses were obtained from a Vario El elemental analyzer. Nitrogen sorption measurements were collected on a Quantachrome Quadrasorb apparatus at 77 K. BET surface areas were determined over a P/P_0 range as described.[11] The samples were degassed at 200 °C for 15 h before measurements. Nonlocal density functional theory (NL-DFT) pore size distributions were determined using the carbon/slit-cylindrical pore model of the Quadrawin software. A Nabertherm L3/11 oven was used as the heating device. Small-angle X-ray scattering (SAXS) measurements were performed in a slit collimation mode with a Kratky camera from Anton Paar Instruments (Graz, Austria). Monochromatized Cu Kα radiation ($\lambda = 1.54$ Å) was used. The measurements were performed at room temperature under vacuum. The scattering vector s is defined by $s = \lambda^{-1} \sin \theta$, with θ being the scattering angle. The scattering patterns were background corrected employing a method described by Perret and Ruland.[12] Calculation of the Porod length l_p was done following known procedures.[12] The interface area S/V is related to l_p by $S/V = 4\varphi(1 - \varphi)l_p^{-1}$, where φ is the porosity of the material. The porosity is calculated from the total pore volume determined by nitrogen sorption and the density of the material, which is calculated according to the literature.[13] The specific surface area is accessible from S/V by taking the material density into account. The number average pore size $\langle l_{pore} \rangle$ is given by $\langle l_{pore} \rangle = l_p(1 - \varphi)^{-1}$.[14]

Transmission electron microscopy (TEM) was carried out with an Omega 912 (Carl Zeiss, Oberkochen, Germany). High-resolution TEM was performed on a Phillips CM 200 FEG electron microscope equipped with a field emission gun. The acceleration voltage was set to 200 kV. The point resolution was 0.2 nm. Electron energy loss spectra (EELS) were recorded with a Gatan Imaging Filter GIF 100 mounted on the CM 200 FEG TEM. The energy resolution was 1 eV full width at half-maximum (fwhm) of the zero loss. Energy-dispersed X-ray spectra were measured on the TEM with an EDXS spectrometer.

Synthesis of the Polytriazine Networks. In a typical experiment, 1,4-dicyanobenzene (1.00 g, 7.8 mmol) and $ZnCl_2$ (5.32 g, 39.0 mmol) were transferred into a quartz ampule (3 × 12 cm) under an inert atmosphere. The ampule was evacuated, sealed, and heated to the desired temperature for different times. The ampule was then cooled to room temperature and opened.

Caution: *For temperatures higher than 500 °C, the ampules are under pressure, which is released during opening.*

The reaction mixture was subsequently ground and then washed thoroughly with water to remove most of the $ZnCl_2$. Further stirring in diluted HCl for 15 h was carried out to remove the residual salt. After this purification step, the resulting black powder was filtered, washed successively with water and THF, and dried in vacuum at 150 °C. Typical isolated yield: 90%.

Results and Discussion

As previously reported, the preparation of the porous polytriazines is carried out conveniently by heating a mixture of the nitrile monomers and zinc chloride in a glass ampule at 400 °C. The polymers can be simply recovered by consecutive washing away the salt from the final mixture with water. The resulting porous material is devoid of residual salts according to EDX elemental analysis (see Supporting Information, Figures S4 and S14). The polytrimerization turned out to be reversible at 400 °C, while higher reaction temperatures (>400 °C) were anticipated to activate additional irreversible reaction pathways in parallel with the nitrile trimerization equilibrium. Indeed, it is well-known that the predominating thermal decomposition pathway of simple, nonfunctional aromatics follows a carbonization process where C−C bonds are formed by C−H bond activation with consecutive H_2 evolution.[15] In addition, we expect for nitriles cleavage of the weakest Ar−CN bonds (for example through homolytic cleavage) as the dominant reaction, leading to direct coupling of neighboring aromatic rings with a typical depletion of nitrogen in the structure as signatures. As zinc chloride boils at 732 °C, 700 °C was the maximal temperature assessed in order to keep the salt in the liquid state. For the present study, 1,4-dicyanobenzene (DCB) was used as a model compound.

The development of the pore system can be nicely followed and quantified by gas sorption experiments. Figure 1 shows the nitrogen adsorption−desorption isotherms and the corresponding pore size distributions of the materials calculated by nonlocal density functional theory (NL-DFT) obtained by polymerizing DCB at different temperatures. Note that the NL-DFT calcula-

(11) Walton, K. S.; Snurr, R. Q. *J. Am. Chem. Soc.* **2007**, *129*, 8552–8556.
(12) Perret, R.; Ruland, W. *Kolloid-Z. Z. Polym.* **1971**, *247*, 835.
(13) Weber, J.; Antonietti, M.; Thomas, A. *Macromolecules* **2008**, *41*, 2880–2885.
(14) *Small Angle X-ray Scattering*; Glatter, O.; Kratky, O., Eds.; Academic Press: London, U.K., 1982; 515 pp.
(15) Johns, I. B.; Smith, J. O.; McElhill, E. A. *Ind. Eng. Chem. Prod. Res. Dev.* **1962**, *1*, 277–281.

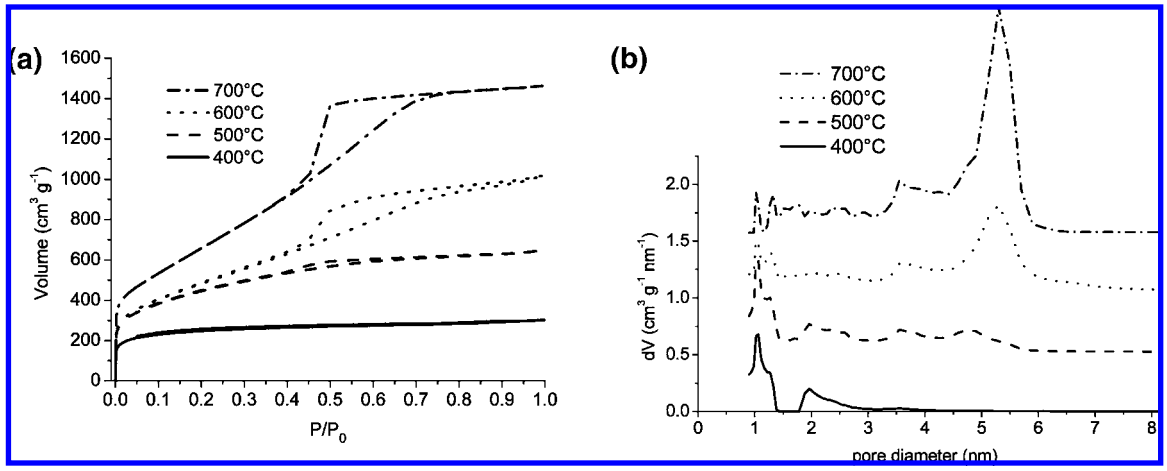

Figure 1. Nitrogen sorption isotherms (A) and NL-DFT pore size distributions (B) of the poly-DCB prepared at different temperatures (ordinate offset 70%). Conditions: 20 h, 5 equiv of $ZnCl_2$.

Table 1. Porous Characteristics of Polytriazines Prepared Using Different Heat Treatments[a]

sample	S_{BET} ($m^2\ g^{-1}$)	S_{SAXS} ($m^2\ g^{-1}$)	total pore volume[b] ($cm^3\ g^{-1}$)	mesopore volume[c] ($cm^3\ g^{-1}$) (%)	average pore diameter (nitrogen sorption) (nm)	average pore diameter (SAXS) (nm)
400[d]	920	1450	0.47	0.16 (34)	2.0	1.5
500[e]	1600	1760	1.00	0.61 (61)	2.5	2.2
600[e]	1750	1800	1.58	1.34 (82)	3.6	3.5
6004d[f]	1930		2.09	1.94 (93)	4.3	
400/600[g]	2660	2410	1.82	1.44 (79)	2.7	3.0
400/6004d[h]	3270		2.4	1.96 (82)	2.9	
700[e]	2530	2600	2.26	2.06 (91)	3.6	3.5

[a] Condition: 5 equiv of $ZnCl_2$. [b] Determined at $P/P_0 = 0.99$. [c] Determined by NL-DFT pore size distribution. [d] At 400 °C, 40 h. [e] At 500, 600, or 700 °C, 20 h. [f] At 600 °C, 96 h. [g] At 400 °C, 20 h; then 600 °C, 20 h. [h] At 400 °C, 20 h; then 600 °C, 96 h.

tions depend strongly on the chemical nature of the surface and on the pore geometries. Here, a model based on carbon with slit/cylindrical pores was chosen as the most reliable, but absolute values still have to be interpreted with care. The expected type I isotherm of purely microporous materials is observed only for the polymer prepared at 400 °C, whereas all samples prepared at higher temperatures exhibit a type IV isotherm with an associated H_2 type hysteresis, indicating the formation of additional mesoporosity.

The slope of the adsorption−desorption curve together with the area of the hysteresis strongly increases with temperature, indicating a growth of the surface area and of the pore volume in the mesopore range. On the other side, the nitrogen uptake at low pressures also rises with the temperature, indicating a gain of the overall surface area. The corresponding quantitative data are summarized in Table 1. As compared to the sample prepared at 400 °C, a remarkable 3-fold increase for surface area and 5-fold increase for pore volume are found for a reaction temperature of 700 °C, reaching respectively 2500 $m^2\ g^{-1}$ and 2.3 $cm^3\ g^{-1}$. The observations on the variation of the pore sizes are further verified by the plots of the NL-DFT pore size distributions. For the sample prepared at 400 °C, the formation of a typical narrow distribution of supermicropores (1−2 nm) is expected due to the dicyanobenzene/triazine system (1.2 nm corresponds to the pore opening of a cyclic hexamer), as previously described in detail elsewhere.[10] When the reaction temperature increases to 500 °C, the system is obviously in a structural transition state, and a broad distribution containing both supermicropores and mesopores is found (between 1 and 6 nm). Further increasing the temperature seems to complete the structural transition, and a well-defined, narrow mesopore population centered at ca. 5.5 nm has developed, while keeping the microporous population typical for the triazine scaffold. Further increase of the temperature up to 700 °C does not further affect the pore size distribution: the structure is now irreversibly fixed.

As determination of the surface area and average pore size by sorption measurements in the supermicropore region is sometimes critical, SAXS measurements were carried out on selected samples. The scattering patterns of all samples showed Porod behavior at high scattering vectors (see Supporting Information, Figure S3). Hence, it was possible to calculate a model-independent number-average pore size as well as the specific surface area on the basis of the SAXS data only.[14] The results are included in Table 1. The average pore sizes are in good agreement with the values obtained by the NL-DFT method. The deviations between the surface areas determined by the BET method and SAXS agree within the experimental error, except for the sample prepared at 400 °C.

For the latter, a significant higher surface area was found by SAXS, which can be explained by the presence of ultramicropores (<0.5 nm) that are not accessible by nitrogen.[16−19]

The evolution of the porosity with the reaction temperature can be correlated with a change of the chemical composition of the porous scaffolds. Figure 2 shows the evolution of the C/N and C/H ratios as a function of the temperature, as measured by combustion elemental analysis (see Supporting Information, Table S1). These data are to be regarded as relative, only, as an average fraction of 17% is "noncombustible" and therefore missing in these measurements. Both ratios slowly grow with the temperature, while at 700 °C the loss of hydrogen and nitrogen is significantly higher. It can be seen that the C/N ratio is more affected by the polymerization temperature than the C/H ratio, indicating that further linkage of the aromatic building blocks presumably occurs mainly via [CN]-elimination, with

(16) Chen, B. L.; Ma, S. Q.; Hurtado, E. J.; Lobkovsky, E. B.; Liang, C. D.; Zhu, H. G.; Dai, S. *Inorg. Chem.* **2007**, *46*, 8705–8709.
(17) Dinca, M.; Long, J. R. *J. Am. Chem. Soc.* **2005**, *127*, 9376–9377.
(18) Dybtsev, D. N.; Chun, H.; Yoon, S. H.; Kim, D.; Kim, K. *J. Am. Chem. Soc.* **2004**, *126*, 32–33.
(19) Ma, S. Q.; Sun, D. F.; Wang, X. S.; Zhou, H. C. *Angew. Chem., Int. Ed.* **2007**, *46*, 2458–2462.

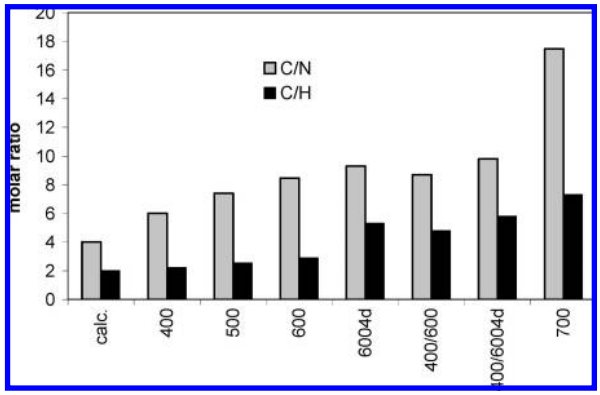

Figure 2. Evolution of C/N and C/H molar ratios of the polymers at different reaction temperatures. Calculated from combustion elemental analysis.

some H_2-elimination in addition. The loss of nitrogen at high temperatures was further confirmed by electron energy loss spectroscopy (EELS; see Supporting Information, Figure S2).

To improve this development of a pore structure on two levels of hierarchy, longer tempering times (sample 6004d), stepwise heating processes (sample 400/600), and a combination of the two (sample 400/6004d) were also assessed. In all those cases the C/H/N ratio remains practically unchanged (see Figure 2), while the connectivity pattern and the related surface area and pore size distribution can indeed be optimized. The final values of surface area and porosity of 3300 $m^2\ g^{-1}$ and 2.4 $cm^3\ g^{-1}$ are to the best of our knowledge the highest ever reached for amorphous organic materials.

These values are even well beyond those of typical carbon blacks,[20,21] and even higher than the hierarchical mesoporous carbons of the CMK-*n* family[22,23] (for example 2300 $m^2\ g^{-1}$ for CMK-5).[22] The surface areas are even in the range of the best metal−organic frameworks (MOFs).[24] For all those samples, the mesopore distribution is broadened, but the surface area is increased up to another 80%, compared to the starting material. The value of 3270 $m^2\ g^{-1}$ is representative of a highly dispersed carbon-like material.[25] Indeed, it overpasses the theoretical surface area of a graphene sheet that is estimated to 2960 $m^2\ g^{-1}$, but is below the calculated surface area of 5680 $m^2\ g^{-1}$ for pure poly-*p*-phenylene.[26]

Figure 3 shows high-resolution TEM pictures of the sample prepared at 700 °C in two different magnifications. Due to the very high porosity, the material is very translucent, but is nevertheless stable against degradation in the electron beam. The porosity and texture are very homogeneous (see Supporting Information, Figures S29 and S30, for TEM pictures), with the walls of the irregular 5 nm pores apparently being formed of two to three sheets of the benzene derived scaffold. The latter is not a dense layer, but is porous in itself. The quantified supermicropores are indeed seen as 1.5 nm spaced spot patterns.

For a structural explanation it must be considered that, even though mesopores are formed during the heat treatment, the surface area increases, which points to the fact that the mesopores are not formed at the cost of, but rather *additionally* to the micropores. According to these results, quite similar networks are formed if the different polymerization reactions (trimerization and carbonizations) occur simultaneously (polymerization at 600 °C) or consecutively (polymerization at 400 °C and then at 600 °C). Schematically, the formation of the defined mesoporosity in the second case can be explained by a retrotrimerization/recombination pathway. The retrotrimerization of the triazines would first form pending cyano-aryl moieties that can then react with other neighboring fragments through irreversible reactions (involving CN-elimination) to fix the created dynamic mesopores. It is in our opinion decisive for this effect that the fragmentation occurs within a dynamic scaffolded structure, where recombination of the building units is not densifying but rather expanding the previous scaffold. In the case where the different reactions occur simultaneously, it can be assumed that a triazine network is formed at an early stage of the reaction and then reorganized, as the trimerization is rather fast and reversible at those temperatures (ca. 600 °C). On the other hand, it is also possible that the simultaneous reversible and irreversible reactions can create secondary in situ formed building units that could rearrange again to quite uniform size building units that are finally irreversibly integrated in the polymer scaffold. In all cases, this complex, self-organizing reaction system leads to a surprisingly well-defined hierarchical porosity.

To further confirm that the polytriazine frameworks can be reorganized and to point out the structure-directing effect of the primary network, an experiment was carried out by heating to 600 °C a mixture of CTF-1 (crystalline sample prepared by polymerizing DCB at 400 °C with 1 mol equiv of $ZnCl_2$)[10] and $ZnCl_2$ under similar conditions. In this case, the surface area of the obtained amorphous network rises to 1540 $m^2\ g^{-1}$ (from 790 $m^2\ g^{-1}$ for CTF-1), a value slightly lower than the 1740 $m^2\ g^{-1}$ found for the material produced from the polymerization of DCB at 600 °C. The pore volume also increases, reaching 1.0 $cm^3\ g^{-1}$ (against 0.4 $cm^3\ g^{-1}$ for CTF-1). Accordingly, much smaller pores are created than for the polymerization of DCB at 600 °C, with an average pore diameter of 1.3 nm, showing that the material formed is mainly microporous (see Supporting Information, Figures S31−S33, for the N_2 isotherm and NL-DFT pore size distribution).

This result clearly illustrates that the dense crystalline network is exerting many more constraints toward the pore expansion. Thus, it appears that any polytriazine network can be reorganized at higher temperatures, and that the structural properties of the final material are directed by the structure of the initial network, in addition to the properties of the monomer.

Conclusions

It was shown that it is possible to create well-defined porous organic materials with a hierarchical pore system, presenting an exceptional high surface area and overall porosity. The key point of their template-free synthesis is a high temperature dynamic polymerization system relying on the use of a salt melt as solvent. The high porosities are reached by a fragmenta-

(20) Rodríguez-Reinoso, F. In *Handbook of porous solids*; Schüth, F.; Sing, K. S. W.; Weitkamp, J., Eds.; Wiley-VCH: Weinheim, Germany, 2002; Vol. 3, pp 1766−1827.
(21) McEnaney, B. In *Handbook of porous solids*; Schüth, F.; Sing, K. S. W.; Weitkamp, J., Eds.; Wiley-VCH: Weinheim, Germany, 2002; Vol. 3, pp 1828−1862.
(22) Lu, A. H.; Li, W. C.; Schmidt, W.; Kiefer, W.; Schuth, F. *Carbon* **2004**, *42*, 2939–2948.
(23) Ryoo, R.; Joo, S. H.; Jun, S. *J. Phys. Chem. B* **1999**, *103*, 7743–7746.
(24) Ferey, G.; Mellot-Draznieks, C.; Serre, C.; Millange, F. *Acc. Chem. Res.* **2005**, *38*, 217–225.
(25) Marsh, H.; Crawford, D.; O'Grady, T. M.; Wennerberg, A. *Carbon* **1982**, *20*, 419–426.
(26) Chae, H. K.; Siberio-Perez, D. Y.; Kim, J.; Go, Y.; Eddaoudi, M.; Matzger, A. J.; O'Keeffe, M.; Yaghi, O. M. *Nature* **2004**, *427*, 523–527.

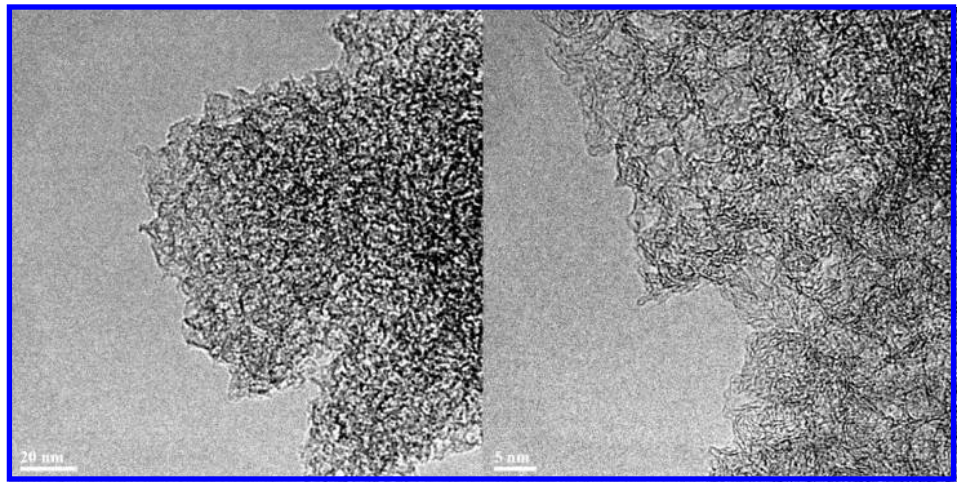

Figure 3. High-resolution TEM pictures of the sample prepared at 700 °C.

tion−recombination mechanism of the structural constituents of the scaffolds. At the same time, the final structure is mechanically, thermally, and chemically rather stable, which is due to the chemical build-up principle and the rather homogeneous texture which involves all the tectonic elements in the mechanical load. In those terms, the present materials can be seen as nitrogen-rich carbonaceous polymers, whose performances are surpassing all currently available commercial activated carbons (partly made with very sophisticated activation schemes), but also all mesoporous carbon replicas of the CMK type. Furthermore, the high nitrogen content found in these materials could yield possible coordination sites for transition metal catalysts.

The most important advantage however comes from the hierarchical structure: contrary to purely microporous materials, such as zeolites or metal−organic frameworks, they combine the advantages of micro- and mesoporous systems; i.e., the structures have an extremely high surface area, but much fewer transport and diffusion restrictions (the micropores are loaded and unloaded via the extended mesopore system, which facilitates transport by orders of magnitude). It is expected that pore blocking of the surface, a critical disadvantage of zeolites, would be practically absent in those structures.

We believe that the present principle can be extended to a wider variety of monomer/polymerization reactions, allowing further tuning of the size of the mesopores, thus making a new generation of materials for gas storage, sorption, and catalyst supports available.

Acknowledgment. This work was supported by the Project House "ENERCHEM" of the Max Planck Society. The authors gratefully acknowledge Dr. Jens Weber for the SAXS measurements and Dr. Frederic Goettmann for fruitful discussions.

Supporting Information Available: TEM images, EDX analysis, elemental analysis, nitrogen adsorption isotherms, BET plots, NL-DFT pore size distributions, SAXS patterns. This material is available free of charge via the Internet at http://pubs.acs.org.

JA803708S